

Article

# Symmetric Assembly of a Sterically Encumbered Allyl Complex: Mechanochemical and Solution Synthesis of the Tris(allyl)beryllate, $K[\text{BeA}'_3]$ ( $\text{A}' = 1,3\text{-(SiMe}_3)_2\text{C}_3\text{H}_3$ )

Nicholas C. Boyde <sup>1</sup>, Nicholas R. Rightmire <sup>1</sup>, Timothy P. Hanusa <sup>1,\*</sup> and William W. Brennessel <sup>2</sup>

<sup>1</sup> Department of Chemistry, Vanderbilt University, Nashville, TN 37235, USA; nicholas.c.boyde@vanderbilt.edu (N.C.B.); nicholas.r.rightmire@vanderbilt.edu (N.R.R.)

<sup>2</sup> Department of Chemistry, University of Rochester, Rochester, NY 14627, USA; william.brennessel@rochester.edu

\* Correspondence: t.hanusa@vanderbilt.edu

Academic Editor: Matthias Westerhausen

Received: 23 April 2017; Accepted: 23 May 2017; Published: 27 May 2017

**Abstract:** The ball milling of beryllium chloride with two equivalents of the potassium salt of bis(1,3-trimethylsilyl)allyl anion,  $K[\text{A}']$  ( $\text{A}' = 1,3\text{-(SiMe}_3)_2\text{C}_3\text{H}_3$ ), produces the tris(allyl)beryllate  $K[\text{BeA}'_3]$  (**1**) rather than the expected neutral  $\text{BeA}'_2$ . The same product is obtained from reaction in hexanes; in contrast, although a similar reaction conducted in  $\text{Et}_2\text{O}$  was previously shown to produce the solvated species  $\text{BeA}'_2(\text{OEt}_2)$ , it can produce **1** if the reaction time is extended (16 h). The tris(allyl)beryllate is fluxional in solution, and displays the strongly downfield  $^9\text{Be}$  NMR shift expected for a three-coordinate Be center ( $\delta 22.8$  ppm). A single crystal X-ray structure reveals that the three allyl ligands are bound to beryllium in an arrangement with approximate  $\text{C}_3$  symmetry ( $\text{Be-C}$  (avg) =  $1.805(10)$  Å), with the potassium cation engaging in cation- $\pi$  interactions with the double bonds of the allyl ligands. Similar structures have previously been found in complexes of zinc and tin, i.e.,  $M[M'A'_3L]$  ( $M' = \text{Zn}, M = \text{Li, Na, K}; M' = \text{Sn}, M = \text{K}; L = \text{thf}$ ). Density functional theory (DFT) calculations indicate that the observed  $\text{C}_3$ -symmetric framework of the isolated anion ( $[\text{BeA}'_3]^-$ ) is  $20 \text{ kJ}\cdot\text{mol}^{-1}$  higher in energy than a  $\text{C}_1$  arrangement; the  $\text{K}^+$  counterion evidently plays a critical role in templating the final conformation.

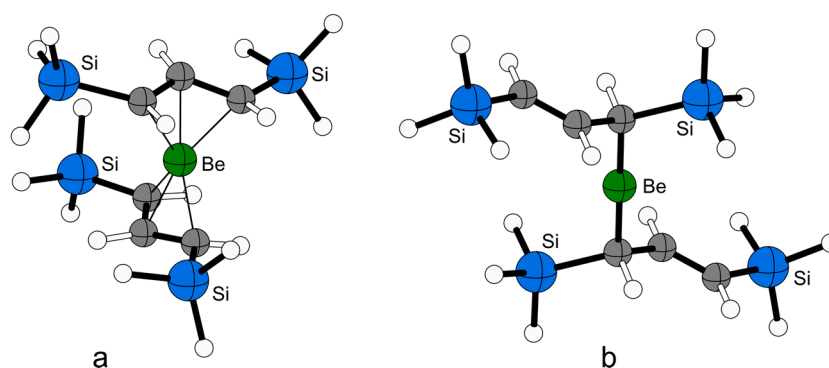
**Keywords:** allyl ligands; beryllium; coordination modes; mechanochemistry; X-ray diffraction; density functional theory calculations

## 1. Introduction

The physical and chemical properties of first-row elements often differ appreciably from their second-row and heavier counterparts; for the group 2 metals, the outlier (“black sheep” [1]) designation belongs to beryllium. To a considerably greater extent than its heavier congeners, even magnesium, the small size of the  $\text{Be}^{2+}$  cation ( $0.27$  Å for CN = 4; cf.  $0.57$  Å for  $\text{Mg}^{2+}$ ) [2] and its corresponding high charge/size ratio ensures its bonds will be strongly polarized and possess substantial covalent character. Not surprisingly, beryllium compounds with the same ligand sets commonly have different structures from those of the other, more electropositive alkaline earth (Ae) metals. The bis(trimethylsilyl)amides of Mg–Ba, for example, have a common dimeric bridged structure,  $[\text{Ae}(\text{N}(\text{SiMe}_3)(\mu\text{-N}(\text{SiMe}_3)_2)_2]$  [3], whereas that of beryllium is a two-coordinate monomer [4]. Similarly, the bis(cyclopentadienyl) complex  $\text{Cp}_2\text{Be}$  has an  $\eta^1, \eta^5\text{-Cp}$  structure [5] that is unlike that of the heavier metallocenes [6]. Investigation of these differences, and indeed research with all beryllium compounds, has traditionally been limited

because of concerns about toxicity [7], but that has not prevented its compounds from serving as useful benchmarks of the steric and electronic consequences of crowded metal environments [8–10].

One of these consequences is the relative stability of  $\eta^1$ - vs.  $\eta^3$ -bonded allyl ligands in compounds of highly electropositive metals. We found some time ago that the bulky allyl  $[A']^-$  ( $A' = [1,3-(\text{SiMe}_3)_2\text{C}_3\text{H}_3]$ ) can be used to form the ether adduct  $\text{Be}A'_2 \cdot \text{OEt}_2$ , which displays  $\eta^1$ -bonded  $A'$  ligands in the solid state [11]. The compound is fluxional in solution, and exhibits symmetric, “ $\pi$ -type” bonding in its NMR spectra (e.g., only one peak is observed for the  $\text{SiMe}_3$  groups). Density functional theory (DFT) calculations suggested that a base-free  $\text{Be}(\text{C}_3\text{H}_3\text{E}_2)_2$  ( $\text{E} = \text{H}, \text{SiH}_3$ ) complex would be more slightly more stable with delocalized,  $\pi$ -type allyls than with monodentate, sigma-bonded ligands (Scheme 1). If so, beryllium allyls would join those of magnesium, in which monodentate allyl ligands are uniformly found in complexes that are ether-solvated [12], but that in the absence of ethers, cation– $\pi$  interactions with the metal can create “slipped- $\pi$ ” bonding [13].



**Scheme 1.** Optimized geometries of  $\text{Be}(1,3-(\text{SiH}_3)_2\text{C}_3\text{H}_3)_2$ . At the B3PW91/aug-cc-pVDZ level, the  $\pi$ -bound structure (a) is  $4.0 \text{ kcal}\cdot\text{mol}^{-1}$  lower in energy ( $\Delta G^\circ$ ) than the  $\sigma$ -bound geometry (b) [11].

The coordinated ether in  $\text{Be}A'_2 \cdot \text{OEt}_2$  proved impossible to remove without destroying the complex [11], and thus we investigated mechanochemical methods of synthesis as a means to bypass the use of ethereal solvents [14]. As detailed below, an unsolvated neutral complex was not isolated via this route, and the beryllate anion that was produced instead has structural parallels with previously described -ate complexes of Zn [15] and Sn [16]. In all of these species, the alkali metal counterion, usually  $\text{K}^+$  but sometimes  $\text{Na}^+$  and  $\text{Li}^+$ , appears to play a critical role in the assembly of the symmetric complexes.

## 2. Results and Discussion

### 2.1. Solid-State Synthesis

The reaction of  $\text{BeCl}_2$  and  $\text{K}[A']$  was conducted mechanochemically with a planetary ball mill, followed by an extraction with hexanes. Initial investigations used 2:1 molar ratios of  $\text{BeCl}_2$  and  $\text{K}[A']$ , based on the assumption that the product formed would be  $\text{Be}A'_2$  (Equation (1)). Although the reagents are off-white ( $\text{K}[A']$ ) and white ( $\text{BeCl}_2$ ), the ground reaction mixture (15 min/600 rpm) is orange. Extraction with hexanes, followed by filtration, yielded an orange filtrate and ultimately a dark orange, highly air-sensitive solid (**1**) on drying.



A single crystal analysis (described below) revealed that **1** is the potassium tris(allyl)beryllate,  $\text{K}[\text{Be}A'_3]$ . This forms in spite of the fact that the 2:1 ratio of reagents used is not optimum for its production. As detailed below, conducting the reaction with 1:1 and 3:1 molar ratios of  $\text{K}[A']$  and  $\text{BeCl}_2$  still yields **1** as the sole hexane-extractable product. It is possible that the excess halide is captured

in the form of polyhalide anions such as  $[\text{BeCl}_4]^{2-}$  or  $[\text{Be}_2\text{Cl}_6]^{2-}$  [17], although these have not been definitively identified.

## 2.2. Synthesis in Solution

The reaction of  $\text{K}[A']$  and  $\text{BeCl}_2$  was also examined in solution, using diethyl ether and hexanes. These results are summarized in Table 1. Previous reactions with diethyl ether involved stirring for 2 h at room temperature, which formed  $\text{BeA}'_2 \cdot \text{OEt}_2$  from a 2:1 reaction (#5); Schlenk equilibrium was observed in a 1:1 mixture that was allowed to react for one hour (#4). When the 2:1 reaction in  $\text{Et}_2\text{O}$  is allowed to proceed for 16 h, however, the formation of **1** is observed (#6) exclusively. Reaction in hexanes mimics the solid-state reactions, in that **1** is the exclusively detected organoberyllium product from a 1:1 reaction after 1 h (#7). Longer reactions and a higher ratio of  $\text{K}[A']$  to  $\text{BeCl}_2$  (e.g., 3:1) do not change this outcome.

**Table 1.** Summary of  $\text{K}[A']$  and  $\text{BeCl}_2$  reactions; amounts of reagents given as molar ratios.

No.	$\text{K}[A']:\text{BeCl}_2$	Medium <sup>a</sup>	Time	Organoberyllium Product(s)	Yield (%) <sup>b</sup>
1	1:1		15 min	$\text{K}[\text{BeA}'_3]$	97
2	2:1		15 min	$\text{K}[\text{BeA}'_3]$	21
3	3:1		15 min	$\text{K}[\text{BeA}'_3]$	25
4	1:1	$\text{Et}_2\text{O}$	1 h	$2A'\text{BeCl} \rightleftharpoons \text{BeA}'_2 + \text{BeCl}$	n/a <sup>c,d</sup>
5	2:1	$\text{Et}_2\text{O}$	2 h	$\text{BeA}'_2 \cdot \text{OEt}_2$	77 <sup>c</sup>
6	2:1	$\text{Et}_2\text{O}$	16 h	$\text{K}[\text{BeA}'_3]$	98
7	1:1	hexanes	1 h	$\text{K}[\text{BeA}'_3]$	24

<sup>a</sup>  = ball milling at 600 rpm. The symbol for mechanical milling has been proposed in ref. [14]; <sup>b</sup> Unrecrystallized; limiting reagent taken into account; <sup>c</sup> Ref. [11]; <sup>d</sup> Products were observed with  $^9\text{Be}$  NMR, and were not isolated.

## 2.3. NMR Spectroscopy

The  $^1\text{H}$  NMR spectrum of **1** displays resonances typical of a “ $\pi$ -bound”  $A'$  ligand, with a triplet representing  $\text{H}_{(\beta)}$ , a broad resonance ( $\nu_{1/2} = 39$  Hz, presumably an unresolved doublet) representing the equivalent  $\text{H}_{(\alpha)}$  and  $\text{H}_{(\gamma)}$ , and a singlet for the two equivalent trimethylsilyl groups (Figure 1). The appearance of such a symmetric spectrum even when  $\sigma$ -bound ligands are expected is consistent with a high degree of fluxionality, as was also observed in the  $\sigma$ -bound complex  $\text{BeA}'_2 \cdot (\text{Et}_2\text{O})$  [11]. The triplet resonance of the allyl ligands, at  $\delta 6.97$ , is shifted downfield from that of  $\text{BeA}'_2 \cdot (\text{Et}_2\text{O})$  ( $\delta 6.53$ ); the resonance at  $\delta 3.19$  is slightly upfield (cf.  $\delta 3.33$  in  $\text{BeA}'_2 \cdot (\text{Et}_2\text{O})$ ). The NMR chemical shifts for **1** are in line with those observed for other  $\text{M}[\text{M}'A'_3]$  complexes (Table 2). In particular, the NMR shifts of the allyl ligands are sensitive both to the identity of the central divalent metal and to that of alkali metal counterion, evidence that the compounds exist as contact ion pairs in solution. Compound **1** and  $\text{K}[\text{ZnA}'_3]$  share the greatest similarities, which may reflect their having the same counterion ( $\text{K}^+$ ) and central metals of similar electronegativity ( $\chi$  Be (1.57); Zn (1.65)) [18].

John and co-workers have demonstrated that  $^9\text{Be}$  NMR chemical shift values can be diagnostic for coordination numbers in solution [19]. Typically, organoberyllium complexes with low formal coordination numbers, such as  $\text{BeMe}_2 \cdot \text{Et}_2\text{O}$  (coordination number 3,  $\delta 20.8$  ppm in  $\text{Et}_2\text{O}$ ), are observed well downfield of 0 ppm.  $\text{BeA}'_2 \cdot (\text{Et}_2\text{O})$  has a  $^9\text{Be}$  chemical shift of  $\delta 18.2$  ppm, which is consistent with a three-coordinate geometry in solution [11]. It should be noted, however, that the correlation between coordination number and  $^9\text{Be}$  chemical shift is not exact, and can be strongly influenced by the electronic properties of the ligands. The 2-coordinate complex beryllium *bis*( $N,N'$ -bis(2,6-diisopropylphenyl)-1,3,2-diazaborolyl), for example, has an extreme downfield shift of  $\delta 44$  ppm [20], whereas the 2-coordinate  $\text{Be}(\text{N}(\text{SiMe}_3)_2)$  displays a  $^9\text{Be}$  NMR shift at  $\delta 12.3$  ppm [4]. Nevertheless, the  $^9\text{Be}$  of **1** is at  $\delta 22.8$  ppm, which to our knowledge is the most positive shift yet reported for a three-coordinate species. DFT methods were used to predict the  $^9\text{Be}$  chemical shift value of **1** (B3LYP-D3/6-311+G(2d,p)//B3LYP-D3/6-31G(d)). It was calculated

at  $\delta 25.9$  ppm, in reasonable agreement with the observed value (referenced to  $[\text{Be}(\text{OH}_2)_4]^{2+}$  with an isotropic shielding constant of 108.98 ppm).

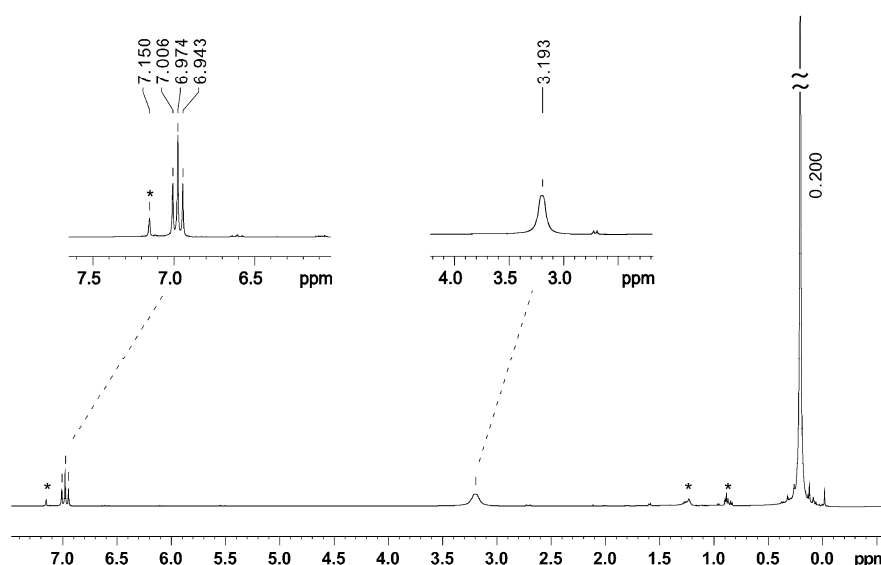


**Figure 1.**  $^1\text{H}$  NMR spectrum (500 Mhz) of isolated **1**, recorded in  $\text{C}_6\text{D}_6$ . The starred peaks represent impurities:  $\delta 7.15$  (residual protons of  $\text{C}_6\text{D}_6$ );  $\delta 0.9$  and  $\delta 1.3$ , residual hexanes.

**Table 2.**  $^1\text{H}$  NMR shifts (ppm) and bond distances in  $\text{M}[\text{M}'\text{A}'_3]$  complexes.

Complex	$\delta \text{H}_{(\alpha)}/\text{H}_{(\gamma)}$	$\delta \text{H}_{(\beta)}$	$\delta \text{SiMe}_3$	M–C ( $\sigma$ ) $\text{\AA}$	M'...C(olefin) $\text{\AA}$	Ref.
Li[ZnA' <sub>3</sub> ]	6.46	3.50	0.15	2.117(3) <sup>b</sup>	2.745(4), 2.268(3) <sup>b</sup>	[15]
Na[ZnA' <sub>3</sub> ]	7.59	4.00	0.16	2.103(3)	2.857(3), 2.567(3)	[15]
K[BeA' <sub>3</sub> ]	6.97	3.19	0.20	1.805(10)	3.153(7), 2.940(7)	this work
K[ZnA' <sub>3</sub> ]	7.05	3.42	0.23	2.068(4)	3.205(3), 2.945(3)	[15]
K(thf)[SnA' <sub>3</sub> ]	6.43	4.42	0.42, 0.23 <sup>a</sup>	2.344(7)	3.201(7), 3.164(8), 3.065(8)	[16]

<sup>a</sup> Two resonances are observed for the  $\text{SiMe}_3$  groups, as the A' ligands are not fluxional; <sup>b</sup> Distance(s) affected by crystallographic disorder.

#### 2.4. Solid State Structure

The structure of **1** was determined from single crystal X-ray diffraction. In the solid state, **1** exhibits approximate  $\text{C}_3$ -symmetry, with  $\sigma$ -bound A' ligands and a potassium cation engaging in cation– $\pi$  interactions with the three double bonds of the allyls. It is isostructural with the previously reported  $\text{M}[\text{ZnA}'_3]$  ( $\text{M} = \text{Li}, \text{Na}, \text{K}$ ) and  $\text{K}(\text{thf})[\text{SnA}'_3]$  complexes [15,16]. The beryllium center is in a nearly planar trigonal environment (sum of C–Be–C' angles =  $357.7^\circ$ ) (Figure 2).

The average Be–C distance of 1.805(10)  $\text{\AA}$  has few direct points of comparison with other molecules, as **1** is only the second crystallographically characterized  $[\text{BeR}_3]^-$  complex, the other being lithium tri-*tert*-butylberyllate [21]. The latter's Be center, like that in **1**, is in a nearly perfectly planar trigonal environment (sum of C–Be–C angles =  $359.9^\circ$ ). In the solid state, however, tri-*tert*-butylberyllate is a dimer,  $[\text{Li}\{\text{Be}(t\text{-C}_4\text{H}_9)_3\}]_2$ , with some corresponding distortions in the Be–C bond lengths; Be–C distances range from 1.812(4)  $\text{\AA}$  to 1.864(4)  $\text{\AA}$ , averaging to 1.843(6)  $\text{\AA}$ . The Be–C length in **1** is indistinguishable from the Be–C<sub>carbene</sub> length of 1.807(4)  $\text{\AA}$  in the  $[\text{Ph}_2\text{Be}(\text{IPr})]$  (IPr = 1,3-bis(2,6-diisopropylphenyl)-imidazol-2-ylidene) complex, which also has a three-coordinate Be center [22]. The anionic methyl groups in  $[\text{Ph}_2\text{Be}(\text{IPr})]$  are at a noticeably shorter distance, however (1.751(6)  $\text{\AA}$ , ave.). A similar relationship between the Be–C<sub>carbene</sub> and Be–CH<sub>3</sub> bond lengths exists in the related  $[\text{Me}_2\text{Be}(\text{IPr})]$  [23] and  $[\text{Me}_2\text{Be}(\text{IMes})]$  (IMes = *N,N'*-bis(2,4,6-trimethylphenyl)imidazol-1-ylidene) complexes [1]. A comparison of the Be–C length in **1** could also be made with the Be–C distance of

1.84 Å in lithium tetramethylberyllate,  $\text{Li}_2[\text{BeMe}_4]$ , although the bond distance would be expected to be slightly longer in the latter owing to the higher coordination number of beryllium and the greater negative charge [24].

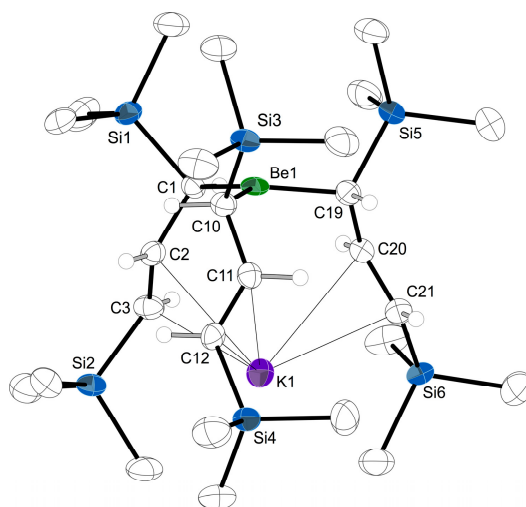


**Figure 2.** Thermal ellipsoid plot of **1**, illustrating the numbering scheme used in the text. Ellipsoids are drawn at the 50% level, and for clarity, hydrogen atoms have been removed from the trimethylsilyl groups. Selected bond distances (Å) and angles (deg): Be1–C1, 1.795(6); Be1–C10, 1.810(6); Be1–C19, 1.811(6); C(2)–C(3), 1.351(5); C(11)–C(12), 1.350(5); C(20)–C(21), 1.358(5); K(1)–C(2), 3.138(4); K(1)–C(3), 2.940(4); K(1)–C(11), 3.206(4); K(1)–C(12), 2.943(4); K(1)–C(20), 3.114(4); K(1)–C(21), 2.938(4); C(1)–Be(1)–C(10), 119.1(3); C(1)–Be(1)–C(19), 119.0(3); C(10)–Be(1)–C(19), 119.4(3).

The C–C and C=C bonds in the alkyl groups in **1** are localized at 1.475(5) Å and 1.353(9) Å, respectively. The  $\text{K}^+\cdots\text{C}$ (olefin) contacts average 3.153(7) Å and 2.940(7) Å to the carbon atoms  $\beta$  (C2, C11, and C20) and  $\gamma$  (C3, C12, and C21) to the beryllium atom, respectively. These distances are comparable to, but slightly shorter than, the range of  $\text{K}^+\cdots\text{C}$  contacts found in the related zincate structure (3.205(3) Å and 2.945(3) Å, respectively), which reflects the shorter M–C( $\alpha$ ) bonds in **1**. The distance between Be and K (3.59 Å) is long enough to rule out significant metal-metal interactions.

### 2.5. Computational Investigations

It has previously been suggested that the occurrence of  $C_3$ -symmetric  $M[M'A'_3L]$  ( $M' = \text{Zn}, M = \text{Li}, \text{Na}, \text{K}; M' = \text{Sn}, M = \text{K}; L = \text{thf}$ ) complexes is the result of a templating effect of the associated alkali metal counterion [25]. The rationale for this proposal is that the neutral  $MA'_3$  ( $M = \text{As}, \text{Sb}, \text{Bi}$ ) complexes always occur in two diastereomeric forms, with  $R,R,R$  (equivalently,  $S,S,S$ ) and  $R,R,S$  (or  $S,S,R$ ) arrangements of the allyl ligands around the central element. The anionic  $[MA'_3]^-$  complexes, in contrast, are always found in the  $C_3$ -symmetric  $R,R,R$  (or  $S,S,S$ ) configuration, and it is not unreasonable to assume that the counterion is responsible for the difference.

A DFT investigation was undertaken to explore the possible origins of this effect. The geometry of the free  $[\text{BeA}'_3]^-$  anion was optimized with calculations employing the dispersion-corrected APF-D functional [26]. Three confirmations were examined: the  $C_3$ -symmetric form ( $S,S,S$ ) found in the X-ray crystal structure of **1**, a related  $S,S,S$  form with one  $A'$  ligand rotated antiparallel to the other two ( $C_1$  symmetry), and a  $R,R,S$  form, also with one ligand antiparallel to the other two, derived from the structure of the neutral  $\text{AlA}'_3$  complex (Figure 3) [27].

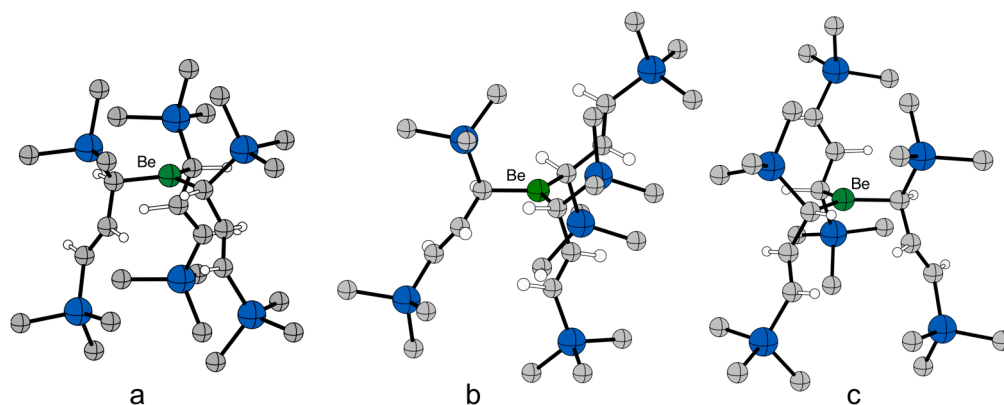


**Figure 3.** Geometry optimized structures of  $[\text{BeA}'_3]^-$  anions: (a) as found in the crystal structure of **1**; (b) related  $S,S,S$  form with one  $A'$  ligand rotated ( $C_1$  symmetry); and (c)  $R,R,S$  form derived from the structure of  $\text{AlA}'_3$ .

Not surprisingly, the calculated structures possess similar average Be–C bond lengths, ranging from 1.782 Å (the  $C_3$ -symmetric form (Figure 3a)) to 1.788 Å (for the rotated  $S,S,S$  form (Figure 3b)). Energetically, the  $R,R,S$  form is the most stable; the rotated  $S,S,S$  form is 10.1  $\text{kJ}\cdot\text{mol}^{-1}$  higher in energy ( $\Delta G^\circ$ ), and the  $C_3$ -symmetric form is higher still (20.3  $\text{kJ}\cdot\text{mol}^{-1}$  in  $\Delta G^\circ$ ). The origin of these energy differences is not immediately obvious, but it may be related to the relative amounts of interligand congestion present. The low energy  $R,R,S$  form, for example, has no  $\text{Me}\cdots\text{Me}'$  contacts less than 4.0 Å, the sum of the van der Waals radii [18]. In contrast, the  $C_3$  symmetric form has multiple contacts between methyl groups of less than 4.0 Å, including two as short as 3.76 Å. At this level of theory, the energetics of the free anions do not provide a rationale for the exclusive formation of the  $S,S,S$  form.

Not surprisingly, incorporation of the  $\text{K}^+$  ion into the complex alters the relative stability of the species. The optimized geometries of the  $C_3$ -symmetric  $\text{K}[\text{BeA}'_3]$  found in the X-ray crystal structure of **1** and a related  $S,S,R$  form were calculated similarly to the isolated anions, and are depicted in Figure 4.

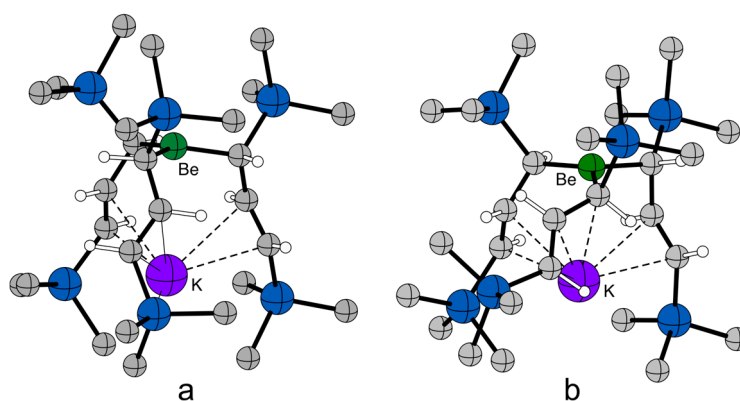


**Figure 4.** Geometry optimized structures of the  $\text{K}[\text{BeA}'_3]$  complex: (a) as found in the crystal structure of **1**; and (b) related  $S,S,R$  form.

The  $C_3$ -symmetric form is 6.1  $\text{kJ}\cdot\text{mol}^{-1}$  more stable than the  $S,S,R$  form. This is not a consequence of closer  $\text{K}^+\cdots(\text{C}=\text{C})$  distances, which are nearly the same (avg. 3.91 Å in the  $C_3$  form; 2.86 Å in the  $S,S,R$  arrangement). The asymmetric arrangement of the ligands in the  $S,S,R$  form does lead to closer interligand  $\text{C}\cdots\text{C}$  contacts in the allyl frameworks, however, as small as 3.37 Å, whereas there are no similar contacts less than 3.78 Å in the  $C_3$  form. The somewhat greater stability of the  $C_3$  form, possibly coupled with greater ease of crystal packing, may contribute to the exclusive appearance of

that form in the crystal structure. It is likely that a similar analysis holds for the isostructural Zn and Sn complexes.

The failure to produce an unsolvated  $\text{BeA}'_2$  in the absence of a coordinating solvent (i.e., either mechanochemically or in hexanes) was also examined computationally with the aid of the Solid-G program [28]. Both  $\text{BeA}'_2 \cdot \text{Et}_2\text{O}$  and **1** are found to have coordination sphere coverage ( $G_{\text{complex}}$ ) above 90% (i.e., 97.0% (Figure 5a) and 92.6% (Figure 5b), respectively). Although the coverage of the metal center in the hypothetical  $\text{BeA}'_2$  varies somewhat with the angle between the ligands, the minimum energy position depicted in Figure 5c ( $C_2$  symmetry) has only 78.7% coverage. It is not unreasonable to assume that a monomeric  $\text{BeA}'_2$  may be too coordinately unsaturated to be readily isolable, and will bind an ethereal solvent molecule during synthesis, or, if that is not available, an additional  $A'$  ligand, counterbalanced with a  $\text{K}^+$  ion.

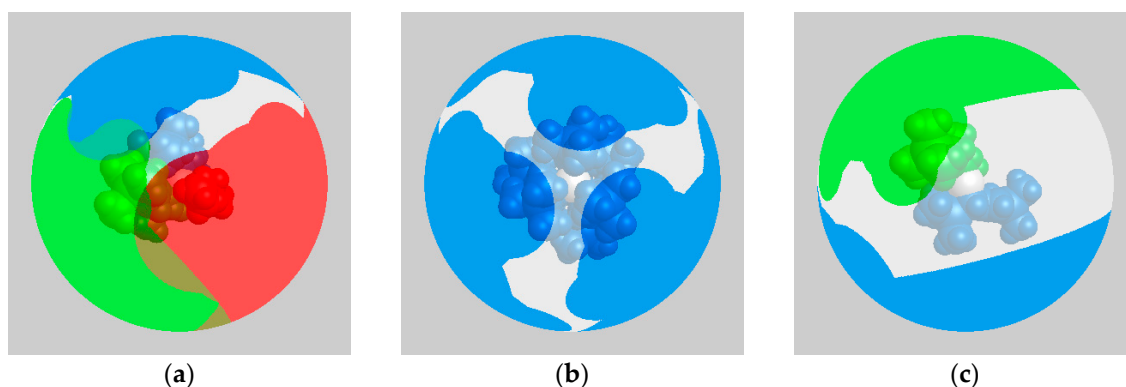


**Figure 5.** Visualization of the extent of coordination sphere coverage ( $G_{\text{complex}}$ ) of: (a)  $\text{BeA}'_2 \cdot \text{Et}_2\text{O}$  (the coverage from the two allyls are assigned blue and green; that from the ether is in red); (b) **1** (all three allyls are in blue); and (c)  $\text{BeA}'_2$ , using optimized coordinates (APF-D/6-311G(2d) (Be); 6-31G(d) (other atoms)) and the program Solid-G [28]. The  $G_{\text{complex}}$  value takes into account the net coverage; regions of the coordination sphere where the projections of the ligands overlap are counted only once.

### 3. Materials and Methods

**General Considerations:** All syntheses were conducted under rigorous exclusion of air and moisture using Schlenk line and glovebox techniques. (NOTE: Beryllium salts are toxic and should be handled with appropriate protective equipment.) After grinding was completed, the jars were opened according to glovebox procedures to protect the compounds and to prevent exposure to dust [10]. Proton ( $^1\text{H}$ ) and carbon ( $^{13}\text{C}$ ) spectra were obtained on Bruker DRX-500 or DRX-400 spectrometers (Karlsruhe, Germany), and were referenced to residual resonances of  $\text{C}_6\text{D}_6$ . Beryllium ( $^9\text{Be}$ ) spectra were obtained on a Bruker DRX-500 at 70.2 MHz, and were referenced to  $\text{BeSO}_4(\text{aq})$ . Combustion analysis was performed by ALS Environmental, Tucson, AZ, USA. Beryllium chloride was purchased from Strem, stored under an  $\text{N}_2$  atmosphere and used as received. The  $\text{K}[A']$  ( $A' = 1,3\text{-(SiMe}_3)_2\text{C}_3\text{H}_3$ ) reagent was synthesized as previously described [29,30]. Toluene, hexanes, and diethyl ether were distilled under nitrogen from potassium benzophenone ketyl [31]. Deuterated benzene ( $\text{C}_6\text{D}_6$ ) was distilled from Na/K (22/78) alloy prior to use. Stainless steel (440 grade) ball bearings (6 mm.) were thoroughly cleaned with hexanes and acetone prior to use. Planetary milling was performed with a Retsch model PM100 mill (Haan, Germany), 50 mL stainless steel grinding jar type C, and safety clamp for air-sensitive grinding.

#### 3.1. Mechanochemical Synthesis of $\text{K}[\text{BeA}'_3]$ (**1**)

Solid  $\text{BeCl}_2$  (56.7 mg, 0.71 mmol) and  $\text{K}[A']$  (319 mg, 1.42 mmol) were added to a 50 mL stainless steel grinding jar (type C). The jar was charged with stainless steel ball bearings (6 mm dia, 50 count) and closed tightly with the appropriate safety closer device under an  $\text{N}_2$  atmosphere. The reagents

were milled for 15 min at 600 rpm, resulting in a light orange solid. The product was extracted under an inert atmosphere with minimal hexanes (<100 mL) and filtered through a medium porosity ground glass frit, providing a dark orange filtrate. Drying under vacuum yielded a dark orange solid (61.5 mg, 21% yield of  $K[BeA'_3]$ ) which was recrystallized by the slow evaporation of toluene over one month to provide dark orange-brown crystals of **1** suitable for single crystal X-ray diffraction. For a 3:1  $K[A']$ : $BeCl_2$  reaction, 812 mg (3.62 mmol)  $K[A']$  and 95.2 mg (1.19 mmol)  $BeCl_2$  were added to a grinding jar. After extraction, 183 mg (25% yield) of orange solid was collected. Anal. Calcd. (%) for  $C_{27}H_{63}BeKSi_6$ : C, 53.65; H, 10.51; Be, 1.49. Found: C, 52.09; H, 9.79; Be, 1.04. The values are somewhat low, possibly from the high air-sensitivity of the compound, but the C:H molar ratio is 2.34:1.00, close to the expected 2.33:1.00.  $^1H$  NMR (500 MHz,  $C_6D_6$ , 298K):  $\delta$  0.20 (s, 54H,  $SiMe_3$ ); 3.19 (br s ( $\nu_{1/2} = 39$  Hz), 6H,  $H_{(\alpha,\gamma)}$ ); 6.97 (t, 3H,  $J_1 = 16$  Hz,  $H_{(\beta)}$ ).  $^{13}C$  NMR (100 MHz,  $C_6D_6$ , 298K):  $\delta$  1.02 (s,  $SiMe_3$ ); 70.71 (s,  $C_{(\alpha,\gamma)}$ ); 166.09 (s,  $C_{(\beta)}$ ).  $^9Be$  NMR (70.2 MHz,  $C_6D_6$ , 298K);  $\delta$  22.8 (s) ( $\nu_{1/2} = 360$  Hz).

### 3.2. General Procedures for Synthesis of $K[BeA'_3]$ (**1**) with Solvents

Reactions were performed for either 1 or 16 h, and were run under inert atmosphere at room temperature. The ratio of  $K[A']$  and  $BeCl_2$  was varied such that the reactions of emphasis were 1:1, 2:1, and 3:1. A general reaction involved dissolving the beryllium chloride (ca. 0.1 g) in the solvent of choice ( $Et_2O$  or hexanes); to this solution solid  $K[A']$  was added slowly and solvent was used to quantitatively transfer all material. Upon mixing, the solution was allowed to stir for the given time. In the case of  $Et_2O$ , the solvent was removed in vacuo, and the resulting material was extracted with hexanes, filtered through a medium porosity glass frit, and then dried in vacuo. In the case of reaction in hexanes, the reaction mixture was filtered through a medium porosity fritted glass filter, and the hexane was removed in vacuo. The resulting material in all cases was then analyzed with  $^1H$  and  $^9Be$  NMR.

### 3.3. Procedures for X-ray Crystallography

A crystal ( $0.20 \times 0.20 \times 0.08$  mm<sup>3</sup>) was placed onto the tip of a thin glass optical fiber and mounted on a Bruker SMART APEX II CCD platform diffractometer (Karlsruhe, Germany) for a data collection at 100.0(5) K [32]. The structure was solved using SIR2011 [33] and refined using SHELXL-2014/7 [34]. The space group  $P\bar{1}$  was determined based on intensity statistics. A direct-methods solution was calculated that provided most non-hydrogen atoms from the E-map. Full-matrix least squares/difference Fourier cycles were performed which located the remaining non-hydrogen atoms. All non-hydrogen atoms were refined with anisotropic displacement parameters. The allylic hydrogen atoms were found from the difference Fourier map and refined freely. All other hydrogen atoms were placed in ideal positions and refined as riding atoms with relative isotropic displacement parameters.

### 3.4. General Procedures for Calculations

All calculations were performed with the Gaussian 09W suite of programs [35]; an ultrafine grid was used for all cases (Gaussian keyword: int = ultrafine). Each conformation of the  $[BeA'_3]^-$  complexes was studied with the APF-D functional, a global hybrid with 23% exact exchange [26]. The 6-31+G(d) basis set was used for C,H,Si; the 6-311+G(2d) basis was used for Be. For the neutral  $K[BeA'_3]$  conformations, the APF-D functional was used with the 6-31G(d) basis set for C,H,Si; 6-311G(2d) was used for Be and K. The nature of the stationary points was determined with analytical frequency calculations; all of these optimized geometries were found to be minima ( $N_{imag} = 0$ ). For the Solid-G calculations, the structures were preoptimized with the APF-D/6-311G(2d) (Be,K); 6-31G(d) (C,H,Si) protocol.

#### 4. Conclusions

The generation of products from reagents that are not in the optimum stoichiometric ratio is a known feature of some Group 2 reactions [36,37], a testament to the role that kinetic factors play in s-block chemistry. It is perhaps not surprising that when mechanochemical activation is used with alkaline earth reagents, a nonstoichiometric product such as the organoberyllate **1** is formed, as grinding and milling environments are often far from equilibrium [38–41]. However, the fact that **1** is also generated in hexanes indicates how non-etheral synthesis can reveal features of reactions that are obscured when they are conducted in coordinating solvents. It is now apparent that the production of the previously described  $\text{BeA}'_2 \cdot \text{Et}_2\text{O}$ , which was the expected complex from a 2:1 reaction of  $\text{K[A}']$  and  $\text{BeCl}_2$  in diethyl ether [11], actually depends critically on the presence of the solvent to prevent further reaction of the beryllium center with an additional  $\text{A}'$  ligand. (In a preliminary study, the reaction of  $\text{K[A}']$  and  $\text{BeCl}_2$  in a 2:1 molar ratio in THF (1 h) was found not to produce  $\text{K[BeA}'_3]$ . A species with a  $^9\text{Be}$  NMR shift of  $\delta 16.6$  ppm was present instead, tentatively identified as  $\text{BeA}'_2(\text{thf})$ . If correct, this indicates that THF, like  $\text{Et}_2\text{O}$ , can block the formation of the tris(allyl) anion with Be). Without such etheral solvent support, whether conducted mechanochemically or in hexanes, the reaction between  $\text{K[A}']$  and  $\text{BeCl}_2$  rapidly forms the kinetic product **1**.

Parallels of the beryllium chemistry to the related tris(allyl) -ate complexes of Zn and Sn are instructive, although they cannot be pushed too far. All the  $[\text{MA}_3]^-$  species possess approximate  $\text{C}_3$  symmetry, and it is likely that the associated alkali metal cation is intimately involved in templating their constructions. The formation of the zinc species  $\text{K[ZnA}'_3]$  is also similar to that of **1** in that it is formed from the reaction of 2 equiv. of  $\text{K[A}']$  and  $\text{ZnCl}_2$ , i.e., in a non-stoichiometric reaction [15]. However, both it and  $\text{K}(\text{thf})[\text{SnA}'_3]$  are synthesized in THF, so it is clear that the driving force for -ate formation compared to that for the neutral  $(\text{Zn}, \text{Sn})\text{A}'_2$  species is greater than that for **1**. This may reflect the somewhat lesser covalency of Be–C versus Zn–C and Sn–C bonds, and the greater robustness of  $\text{M}^{2+} \leftarrow \text{:OR}_2$  interactions with beryllium.

**Supplementary Materials:** The following are available online at <http://www.mdpi.com/2304-6740/5/2/36/s1>: CIF and checkCIF file, and fractional coordinates of geometry-optimized structures.

**Acknowledgments:** Financial support by the National Science Foundation (CHE-1112181), The American Chemical Society–Petroleum Research Fund (56027-ND3), and a Discovery Grant of Vanderbilt University is gratefully acknowledged.

**Author Contributions:** The project concept was devised equally by all authors. Nicholas C. Boyde and Nicholas R. Rightmire performed the experiments and analyzed the resulting data. William W. Brennessel obtained and solved the single crystal X-ray data. The manuscript was written by Timothy P. Hanusa, with contributions from all the co-authors.

**Conflicts of Interest:** The authors declare no conflict of interest.

#### References

1. Arrowsmith, M.; Hill, M.S.; Kociok-Köhn, G. Activation of *N*-Heterocyclic Carbenes by  $\{\text{BeH}_2\}$  and  $\{\text{Be}(\text{H})(\text{Me})\}$  Fragments. *Organometallics* **2015**, *34*, 653–662. [CrossRef]
2. Shannon, R.D. Revised effective ionic radii and systematic studies of interatomic distances in halides and chalcogenides. *Acta Crystallogr. Sect. A* **1976**, *32*, 751–767. [CrossRef]
3. Westerhausen, M. Synthesis and Spectroscopic Properties of Bis(trimethylsilyl)amides of the Alkaline-earth Metals Magnesium, Calcium, Strontium, and Barium. *Inorg. Chem.* **1991**, *30*, 96–101. [CrossRef]
4. Naglav, D.; Neumann, A.; Blaser, D.; Wolper, C.; Haack, R.; Jansen, G.; Schulz, S. Bonding situation in  $\text{Be}[\text{N}(\text{SiMe}_3)_2]_2$ —An experimental and computational study. *Chem. Commun.* **2015**, *51*, 3889–3891. [CrossRef] [PubMed]
5. Nugent, K.W.; Beattie, J.K.; Hambley, T.W.; Snow, M.R. A precise Low-temperature crystal structure of bis(cyclopentadienyl)beryllium. *Aust. J. Chem.* **1984**, *37*, 1601–1606. [CrossRef]
6. Burkey, D.J.; Hanusa, T.P. Structural Lessons from Main-Group Metallocenes. *Comments Inorg. Chem.* **1995**, *17*, 41–77. [CrossRef]

7. Civic, T.M. Beryllium Metal Toxicology: A Current Perspective. In *Encyclopedia of Inorganic and Bioinorganic Chemistry*; John Wiley & Sons, Ltd.: Hoboken, NJ, USA, 2011.
8. Hanusa, T.P.; Bierschenk, E.J.; Engerer, L.K.; Martin, K.A.; Rightmire, N.R. 1.37—Alkaline Earth Chemistry: Synthesis and Structures. In *Comprehensive Inorganic Chemistry II*, 2nd ed.; Reedijk, J., Poeppelemeier, K., Eds.; Elsevier: Amsterdam, The Netherlands, 2013; pp. 1133–1187.
9. Iversen, K.J.; Couchman, S.A.; Wilson, D.J.D.; Dutton, J.L. Modern organometallic and coordination chemistry of beryllium. *Coord. Chem. Rev.* **2015**, *297–298*, 40–48. [[CrossRef](#)]
10. Naglav, D.; Buchner, M.R.; Bendt, G.; Kraus, F.; Schulz, S. Off the Beaten Track—A Hitchhiker’s Guide to Beryllium Chemistry. *Angew. Chem. Int. Ed.* **2016**, *55*, 10562–10576. [[CrossRef](#)] [[PubMed](#)]
11. Chmely, S.C.; Hanusa, T.P.; Brennessel, W.W. Bis(1,3-trimethylsilylallyl)beryllium. *Angew. Chem. Int. Ed.* **2010**, *49*, 5870–5874. [[CrossRef](#)] [[PubMed](#)]
12. Solomon, S.A.; Murny, C.A.; Layfield, R.A. s-Block metal complexes of a bulky, donor-functionalized allyl ligand. *Chem. Commun.* **2008**, 3142–3144. [[CrossRef](#)] [[PubMed](#)]
13. Chmely, S.C.; Carlson, C.N.; Hanusa, T.P.; Rheingold, A.L. Classical versus Bridged Allyl Ligands in Magnesium Complexes: The Role of Solvent. *J. Am. Chem. Soc.* **2009**, *131*, 6344–6345. [[CrossRef](#)] [[PubMed](#)]
14. Rightmire, N.R.; Hanusa, T.P. Advances in Organometallic Synthesis with Mechanochemical Methods. *Dalton Trans.* **2016**, *45*, 2352–2362. [[CrossRef](#)] [[PubMed](#)]
15. Gren, C.K.; Hanusa, T.P.; Rheingold, A.L. Threefold Cation– $\pi$  Bonding in Trimethylsilylated Allyl Complexes. *Organometallics* **2007**, *26*, 1643–1649. [[CrossRef](#)]
16. Layfield, R.A.; Garcia, F.; Hannauer, J.; Humphrey, S.M. Ansa-tris(allyl) complexes of alkali metals: Tripodal analogues of cyclopentadienyl and ansa-metallocene ligands. *Chem. Commun.* **2007**, 5081–5083. [[CrossRef](#)] [[PubMed](#)]
17. Neumüller, B.; Weller, F.; Dehnicke, K. Synthese, Schwingungsspektren und Kristallstrukturen der Chloroberyllate  $(\text{Ph}_4\text{P})_2[\text{BeCl}_4]$  und  $(\text{Ph}_4\text{P})_2[\text{Be}_2\text{Cl}_6]$ . *Z. Anorg. Allg. Chem.* **2003**, *629*, 2195–2199. [[CrossRef](#)]
18. Allred, A.L. Electronegativity values from thermochemical data. *J. Inorg. Nucl. Chem.* **1961**, *17*, 215–221. [[CrossRef](#)]
19. Plieger, P.G.; John, K.D.; Keizer, T.S.; McCleskey, T.M.; Burrell, A.K.; Martin, R.L. Predicting  $^9\text{Be}$  Nuclear Magnetic Resonance Chemical Shielding Tensors Utilizing Density Functional Theory. *J. Am. Chem. Soc.* **2004**, *126*, 14651–14658. [[CrossRef](#)] [[PubMed](#)]
20. Arnold, T.; Braunschweig, H.; Ewing, W.C.; Kramer, T.; Mies, J.; Schuster, J.K. Beryllium bis(diazaborolyl): Old neighbors finally shake hands. *Chem. Commun.* **2015**, *51*, 737–740. [[CrossRef](#)] [[PubMed](#)]
21. Wermer, J.R.; Gaines, D.F.; Harris, H.A. Synthesis and molecular structure of lithium tri-*tert*-butylberyllate,  $\text{Li}[\text{Be}(\text{tert-C}_4\text{H}_9)_3]$ . *Organometallics* **1988**, *7*, 2421–2422. [[CrossRef](#)]
22. Gottfriedsen, J.; Blaurock, S. The First Carbene Complex of a Diorganoberyllium: Synthesis and Structural Characterization of  $\text{Ph}_2\text{Be}(i\text{-Pr-carbene})$  and  $\text{Ph}_2\text{Be}(n\text{-Bu}_2\text{O})$ . *Organometallics* **2006**, *25*, 3784–3786. [[CrossRef](#)]
23. Arrowsmith, M.; Hill, M.S.; Kociok-Köhn, G.; MacDougall, D.J.; Mahon, M.F. Beryllium-Induced C–N Bond Activation and Ring Opening of an *N*-Heterocyclic Carbene. *Angew. Chem. Inter. Ed.* **2012**, *51*, 2098–2100. [[CrossRef](#)] [[PubMed](#)]
24. Weiss, E.; Wolfrum, R. Über metall-alkyl-verbindungen VIII. Die kristallstruktur des lithium-tetramethylberyllats. *J. Organomet. Chem.* **1968**, *12*, 257–262. [[CrossRef](#)]
25. Rightmire, N.R.; Bruns, D.L.; Hanusa, T.P.; Brennessel, W.W. Mechanochemical Influence on the Stereoselectivity of Halide Metathesis: Synthesis of Group 15 Tris(allyl) Complexes. *Organometallics* **2016**, *35*, 1698–1706. [[CrossRef](#)]
26. Austin, A.; Petersson, G.A.; Frisch, M.J.; Dobek, F.J.; Scalmani, G.; Throssell, K. A Density Functional with Spherical Atom Dispersion Terms. *J. Chem. Theory Comp.* **2012**, *8*, 4989–5007. [[CrossRef](#)] [[PubMed](#)]
27. Rightmire, N.R.; Hanusa, T.P.; Rheingold, A.L. Mechanochemical Synthesis of  $[\text{1,3-(SiMe}_3)_2\text{C}_3\text{H}_5]_3(\text{Al,Sc})$ , a Base-Free Tris(allyl)aluminum Complex and Its Scandium Analogue. *Organometallics* **2014**, *33*, 5952–5955. [[CrossRef](#)]
28. Guzei, I.A.; Wendt, M. An improved method for the computation of ligand steric effects based on solid angles. *Dalton Trans.* **2006**, 3991–3999. [[CrossRef](#)] [[PubMed](#)]
29. Fraenkel, G.; Chow, A.; Winchester, W.R. Dynamics of solvated lithium(+) within *exo,exo*-[1,3-bis(trimethylsilyl)allyl]lithium *N,N,N',N'*-tetramethylethylenediamine complex. *J. Am. Chem. Soc.* **1990**, *112*, 1382–1386. [[CrossRef](#)]

30. Harvey, M.J.; Hanusa, T.P.; Young, V.G., Jr. Synthesis and Crystal Structure of a Bis(allyl) Complex of Calcium,  $[\text{Ca}\{\text{C}_3(\text{SiMe}_3)_2\text{H}_3\}_2 \cdot (\text{thf})_2]$ . *Angew. Chem. Int. Ed.* **1999**, *38*, 217–219. [[CrossRef](#)]
31. Perrin, D.D.; Armarego, W.L.F. *Purification of Laboratory Chemicals*, 3rd ed.; Pergamon: Oxford, UK, 1988.
32. APEX2; Version 2014.11-0; Bruker AXS: Madison, WI, USA, 2013.
33. Burla, M.C.; Caliendo, R.; Camalli, M.; Carrozzini, B.; Cascarano, G.L.; Giacovazzo, C.; Mallamo, M.; Mazzone, A.; Polidori, G.; Spagna, R. *SIR2011: A New Package for Crystal Structure Determination and Refinement*; Version 1.0; Istituto di Cristallografia: Bari, Italy, 2012.
34. Sheldrick, G.M. *SHELXL-2014/7*; University of Göttingen: Göttingen, Germany, 2014.
35. Frisch, M.J.; Trucks, G.W.; Schlegel, H.B.; Scuseria, G.E.; Robb, M.A.; Cheeseman, J.R.; Scalmani, G.; Barone, V.; Mennucci, B.; Petersson, G.A.; et al. *Gaussian 09W*; Revision D.01; Gaussian, Inc.: Wallingford CT, USA, 2009.
36. Glock, C.; Görls, H.; Westerhausen, M. *N,N,N',N'*-Tetramethylethylenediamine adducts of amido calcium bases—Synthesis of monomeric  $[(\text{tmeda})\text{Ca}\{\text{N}(\text{SiMe}_3)_2\}_2]$ ,  $[(\text{tmeda})\text{Ca}\{\text{NiPr}_2\}_2]$ , and dimeric Hauser base-type  $[(\text{tmeda})\text{Ca}(\text{tmp})(\mu\text{-I})_2]$  ( $\text{tmp} = 2,2,6,6$ -tetramethylpiperidide). *Inorg. Chim. Acta* **2011**, *374*, 429–434. [[CrossRef](#)]
37. Fitts, L.S.; Bierschenk, E.J.; Hanusa, T.P.; Rheingold, A.L.; Pink, M.; Young, V.G. Selective modification of the metal coordination environment in heavy alkaline-earth iodide complexes. *New J. Chem.* **2016**, *40*, 8229–8238. [[CrossRef](#)]
38. Hernández, J.G.; Friščić, T. Metal-catalyzed organic reactions using mechanochemistry. *Tetrahedron Lett.* **2015**, *56*, 4253–4265. [[CrossRef](#)]
39. Boldyreva, E. Mechanochemistry of inorganic and organic systems: What is similar, what is different? *Chem. Soc. Rev.* **2013**, *42*, 7719–7738. [[CrossRef](#)] [[PubMed](#)]
40. Wang, G.-W. Mechanochemical organic synthesis. *Chem. Soc. Rev.* **2013**, *42*, 7668–7700. [[CrossRef](#)] [[PubMed](#)]
41. Waddell, D.C.; Thiel, I.; Clark, T.D.; Marcum, S.T.; Mack, J. Making kinetic and thermodynamic enolates via solvent-free high speed ball milling. *Green Chem.* **2010**, *12*, 209–211. [[CrossRef](#)]



© 2017 by the authors. Licensee MDPI, Basel, Switzerland. This article is an open access article distributed under the terms and conditions of the Creative Commons Attribution (CC BY) license (<http://creativecommons.org/licenses/by/4.0/>).